Two-Dimensional Electron Spin Resonance and Slow Motions

Sunil Saxena[†] and Jack H. Freed*

Baker Laboratory of Chemistry, Cornell University, Ithaca, New York 14853-1301

Received: May 22, 1997; In Final Form: August 12, 1997[⊗]

The slow rotational dynamics of a polyproline peptide with a nitroxide labeled at one end in a glassy medium is probed using two-dimensional (2D) electron spin resonance (ESR). The contributions to the homogeneous relaxation time, T_2, from the overall and/or the internal rotations of the nitroxide is elucidated from the COSY spectra. The use of pure absorption spectra allows the variation of T_2 across the spectrum to be monitored. It is shown from simulations that the model of anisotropic Brownian diffusion provides semiquantitative agreement with such a variation. In the 2D ELDOR experiment several mechanisms can lead to spectral diffusion, which yields a broadening of the hyperfine (hf) auto-peaks with mixing time. We call these spectral diffusion (SD) cross-peaks. It is shown that at higher temperatures the principal mechanism for the formation of SD cross-peaks is the slow reorientation of the molecule, which modulates the ^{14}N hf and g tensor interactions. A procedure is shown for extracting a correlation time, τ_c, by monitoring this growth of SD cross-peaks, which is in good agreement with theory. An anomalous temperature dependence of the experimental τ_c, at very low temperatures, is tentatively attributed to the fast internal rotations of the methyl groups on the nitroxide, which leads to spin-flips of the protons on these methyl groups. The use of pure absorption spectra in 2D ELDOR enhances the sensitivity to these cross-peaks.

Introduction

The study of inter- and intramolecular motions in the slow motional regime is an important area of research. Many samples of interest such as glassy fluids, polymers, and proteins naturally tumble at rates that lead to slow motional line shapes in electron spin resonance (ESR). There is considerable interest in the determination of the rotational motions by ESR, in order to provide insights into the rates and mechanisms of dynamics in these systems. Most investigations have, however, been limited to continuous wave (CW) ESR where the line shapes are often dominated by the inhomogeneous contributions to the line width, (i.e. T_2^*). However, electron spin−echo (ESE) spectroscopy enables the cancellation of inhomogeneous broadening, so that the homogeneous line widths, given by the inverse phase memory time, T_M^{-1} (which we will call T_2^{-1} for simplicity), can be studied.[1−3] In the slow motional regime the T_2 for a nitroxide is typically 15−500 ns at 9.5 GHz, while T_2^* can be as small as 5−10 ns. The T_2 is typically at least an order of magnitude longer than T_2^*, and one finds that this extends the capability of ESR for measuring slower rotations characterized by rates on the order of 1×10^4 s^{-1}.

However, the analysis is complicated by the fact that the T_2 decay time can include contributions from many processes that lead to a dephasing of the electron spins.[4,5] For example, in a nitroxide, these processes may include (a) the modulation of the g and hyperfine (hf) terms due to the reorientation of the nitroxide moiety by the tumbling of the molecule as a whole and/or by internal molecular motions,[4,6,7] (b) spin−spin relaxation between the observed spin and matrix nuclear spins[8] (or between other electron spins present in the sample[9,10]), (c) modulation of the dipolar interaction between the methyl protons on the nitroxide moiety and the electron spin due to internal rotations of the methyl group,[11−13] and (d) in a biradical, spin

relaxation induced by modulation of the electron−electron dipolar interaction.[14] In this regime, mechanism a is of primary interest to us for the elucidation of motional dynamics.

To delineate these contributions, one needs the extra resolution provided by two-dimensional (2D) ESR (COSY, SECSY, and 2D ELDOR), wherein the different relaxation processes can be further separated using two orthogonal frequency dimensions, and also cross-relaxation (which reports on rotational and translational rates, cf. below) can be monitored. We therefore discuss these two important advantages further, with the aim of clarifying how they relate to the study of motional dynamics, and we also compare these modern 2D techniques to other traditional echo-based approaches used for the purpose of studying slow motions.

In the two-pulse SECSY ESR[15−17] experiment, the first pulse creates x−y magnetization, which gets frequency labeled during a period of evolution, t_1. The second pulse reverses this magnetization during the collection period, t_2, so that the inhomogeneous broadenings are canceled at $t_2 = t_1$. The full 2D frequency spectrum then provides the inhomogeneously broadened CW-equivalent spectra along the f_2 domain, while the homogeneous line shapes appear along the f_1 domain, thereby providing a clean separation of these broadenings.

In principle, the field swept (FS) 2D ESE experiment[18,19] also provides a measurement of T_2 as a function of resonant magnetic field B_0 (and hence frequency). However, the FS-2D ESE experiment is more time consuming, since it lacks the *multiplexing* advantage of the true Fourier transform (FT) SECSY/COSY experiment. Note also, that the FS-2D ESE experiment is based on weak (selective) pulses of long duration (≈60 ns), whereas the SECSY experiment is typically performed using strong pulses of about 5 ns duration. The long selective pulse will therefore contribute to the effective dead-time[20] of the experiment, so it precludes the study of shorter T_2's.[18]

Also the information content in the two experiments can be subtly different. For example, in the slow motional regime an ESR spectrum consists of many complex Lorentzians referred to as "dynamic spin packets".[6,7] In a 2D experiment there can

---
* To whom correspondence should be addressed. Email: *jhf@msc.cornell.edu.* Fax: (607) 255-0595.
† Current address: Chemical Engineering, California Institute of Technology, Pasadena, CA 91125.
⊗ Abstract published in *Advance ACS Abstracts,* October 1, 1997.

be interference between them, which arises from the way they are affected by the second (or "refocusing") pulse in the SECSY experiment. That is, this refocusing pulse can lead to some interchanges between the dynamic spin packets. The selective excitation of the FS-2D ESE leads to interference between only those "dynamic spin packets" resonating at nearly the same frequency,[6] whereas the SECSY experiment involving simultaneous irradiation of the whole spectrum can lead to more extensive interference among the "dynamic spin packets" in the slow motional spectrum.

In the slow motional regime, the T_2's were found to vary across the FS-2D ESE spectrum, reflecting effects due to molecular orientational dynamics.[18,19] Millhauser and Freed[18] showed from spectral simulations that the variation in T_2 across the spectrum could be used to distinguish between models of molecular reorientation based on Brownian, jump, and free diffusion. The experimental data for a relatively small nitroxide in a glassy medium, in the temperature range 173−208 K, fit best to the model of nearly isotropic Brownian diffusion. Dzuba et al.[19] later showed that such field dependences of T_2 at 77 K (where the overall molecular motions are expected to be quenched) could be fit to a solid-state model involving low-amplitude torsional motions of a molecule about its equilibrium position in the solid. However, the latter mechanism would lead to a "motional narrowing" type of relaxation and *not* a slow motional relaxation. These distinctions have been discussed in the context of 2D ESR by Lee et al.[21] Lee et al.[22] illustrate how 2D ESR may be used to distinguish between such possibilities. Another straightforward way is by observing the temperature dependence of T_2. In the motional narrowing case $T_2 \propto \tau_c^{-1}$, where τ_c is the correlation time for the motion, so that T_2 will typically decrease with decreasing temperature. However, for the slow motional case, $T_2 \propto (\tau_c)^\alpha$ with $1 \leq \alpha \leq 1/2$ so that T_2 typically increases with decreasing temperature,[3,6] as was found by Millhauser and Freed.[18]

We note that, in principle, the SECSY experiment provides the same information, and in fact the variation of T_2 across the spectrum forms an effective method for extracting the contribution of molecular dynamics to T_2, (i.e. mechanism a, cf. above) from the other processes (i.e. mechanisms b, c, and d, cf. above).

The epitome of 2D ESR experiments is 2D ELDOR.[15−17] This consists of a three-pulse sequence in which the first pulse creates transverse magnetization that evolves for a period, t_1. A second pulse transfers this frequency-labeled magnetization into z magnetization where magnetization transfer (MT) can occur for a duration of time (called the mixing time), T_M. Finally, the third pulse re-creates transverse magnetization which is experimentally observed during a period, t_2. The signal is typically collected vs t_2 for a series of steps in t_1 and for a fixed duration of the mixing time. Magnetization transfer during the mixing time causes spins precessing at a frequency "f_a" during t_1 to precess at a different frequency "f_b" during t_2, leading to the formation of cross-peaks in the 2D ESR frequency domain spectrum. Usually, the 2D experiment is performed for a series of values of the mixing time, T_M, to directly probe this growth of cross-peaks. Note that the COSY/SECSY experiments correspond to the zero mixing time (i.e. $T_M = 0$) 2D ELDOR experiment.

For $T_M > 0$, cross-peaks can develop in the 2D ESR spectra, which enables the direct elucidation of different relaxation mechanisms and dynamics. The principle mechanisms for MT in nitroxides in the fluid phases are (1) rotational modulation of the electron−nuclear dipolar interaction (END) between electron spin and the nitrogen nucleus and (2) Heisenberg spin exchange (HE) between colliding radical pairs. As motions slow down, the latter becomes superseded by the electron−electron

dipolar (EED) interactions between the colliding radical pairs. In 2D ELDOR these interactions lead to the formation of distinct "off-diagonal" cross-peaks (usually called first- and second-order cross-peaks), correlating the different hyperfine (hf) auto-peaks.[15−17]

In the very slow motional regime another class of cross-peaks become relevant.[22] Each point in f_2 consists of contributions to the signal from an orientation or a set of orientations of the nitroxide with respect to the dc magnetic field. The "real-time" reorientation of the molecule during the mixing time, T_M, leads to a transfer of magnetization from one resonant frequency in f_1 to another in f_2, thereby leading to "rotational cross-peaks". Since the number of orientations with respect to the dc magnetic field provides a continuum, this mechanism leads to a broadening of the auto-peaks themselves. The measurement of this broadening of auto-peaks as a function of mixing time is then a measure of the "real-time" dynamics of the molecule. Since this mechanism provides a form of spectral diffusion (SD), these cross-peaks will also be referred to as spectral diffusion (SD) cross-peaks.

Note that the modulation of the dipolar interaction between methyl protons on the nitroxide moiety and the electron spin due to the internal rotation of these methyl groups[11] can also provide a mechanism for SD cross-peaks. Additionally, the interaction of the electron spin with matrix protons[11,21,23] in the glassy environment can also contribute a small amount to the SD cross-peaks.

Some earlier work on elucidating reorientational dynamics in glassy liquids has focused on the measurement of the MT by saturating a small component, "f_a " (using a π pulse), of the ESR spectrum and measuring the time kinetics of saturation transfer to another component "f_b" using a rapid stepping of the magnetic field and a two-pulse echo sequence.[11,17,24,25] We refer to this as a "hole-burning" experiment. The work of Dzuba et al. was interpreted in terms of dynamics of the nitroxides in glassy liquids, which execute large angle jumps[11] and/or jumps between two fixed orientations of unequal probabilities,[24] since they were otherwise inconsistent with models based on continuous diffusion.[11] Hornak and Freed,[25] who called the technique FS-SE-ELDOR, initially interpreted their results in terms of large angle reorientational jumps, but Schwartz et al.[26] later showed that a more likely interpretation is in terms of an "orientation-independent" nuclear spin-flip[26,27] mechanism. This is consistent with the first 2D ELDOR experiments in glassy fluids[28] and saturation-recovery experiments of Robinson and co-workers.[29] Because of the severe limitations of the "hole-burning" technique, its application was limited to very low temperatures and very viscous fluids corresponding to long relaxation times.

Note that while the 2D ELDOR experiment, like the "hole-burning" experiment, allows the display of not only where the magnetization arose but also where it was finally delivered, it accomplishes this in one simple time-efficient experiment. The 2D ELDOR experiment contains the *multiplexing* advantage of FT spectroscopy, and hence a full 2D collection, involving the simultaneous irradiation, as well as MT from (and to) all positions in the spectrum, typically takes about 15−20 min with current technology. At a given temperature one usually collects 6−10 2D experiments at different values of the mixing time, T_M. In the analogous "hole-burning" experiment one would need to step out both "f_a" and "f_b" in a 2D fashion, as well as T_M, to reconstruct the information provided by the ELDOR experiment(s). Further, the 2D ELDOR experiment obviates the need for a rapid field step. The use of long pulses and field stepping restricts the "hole-burning" experiment to slower rates,

whereas the 2D ELDOR is applicable to virtually the entire motional regime.

Further, the 2D ELDOR experiment allows the clean study of SD cross-peaks, since they appear separated from the END/HE-induced single and double-order cross-peaks. In principle, the "hole-burning" experiment allows this, but the filling of the "hole" due to MT has contributions from all processes, and a detailed analysis is required to distinguish the contributions.[11] The study of the growth of SD cross-peaks in 2D ELDOR allows the monitoring of superslow reorientational dynamics, even in cases where the dynamics is slow enough that it cannot be studied using the homogeneous T_2's.[22]

The rigorous theory for the "hole-burning" experiment depends on the details of the pulse shapes, while that for the 2D ELDOR experiment is simpler especially in the limit of very strong pulses.[22] However, note that as mentioned above (for the case of SECSY vs FS-2D ESE) the hole-burning experiment might contain a smaller degree of interference among the "dynamic spin packets" than the 2D ELDOR experiment.

Finally, we note that the most sensitive 2D ESR method for the elucidation of dynamics is by analyzing the pure absorption 2D ELDOR line shapes,[30] which requires correction for phase[30] variations, introduced due to finite pulses and dead-times. Such phase corrections are typically not needed for the "hole-burning" experiment.

The quantitative analysis of slow motional spectra relies on theoretical simulations based on the stochastic Liouville equation (SLE).[27,31] The general procedure involves the expansion of the stochastic Liouville operator in terms of a suitable basis set,[6,22,27,31] (usually a direct product of the spin basis vectors and Wigner rotation matrixes). In the slow motional regime however, the dimensions of the basis vectors become very large, providing a substantial challenge for simulating slow motional 2D ESR spectra. One approach for obviating the need for a full simulation is to develop simple methods for estimating the rotational correlation times from slow motional spectra,[22,32] and this is one of the objectives of the present study.

Thus, the full analysis of very slow motional 2D ESR spectra is complex. This paper presents an attempt at elucidating the different relaxation mechanisms using slow motional 2D ESR. For this purpose the COSY/SECSY and 2D ELDOR experiments were performed on a monoradical and a biradical in a glass-forming environment. In particular, we utilized labeled polyproline peptides that were available from our previous 2D ESR study of double-quantum coherences.[33] The key experimental details are provided in the Experimental Section. The use of pure absorption line shapes significantly enhances the sensitivity of 2D ESR for studying slow dynamics. A brief summary of the method used to theoretically obtain such absorption slow motional line shapes is provided in the Theory section. Also, the approximations that provide a curtailment of interference between the "dynamic spin packets" (cf. above) in 2D FS ESE are recapitulated. It is shown how T_2 variations across the spectrum in the COSY/SECSY can be used to elucidate motional rates and mechanism in the Results and Discussion section. Also, the cross-peak formation in the 2D ELDOR experiment is used to distinguish between different cross-relaxation mechanisms and for easily extracting a correlation time from the experiment. The main results are outlined in the Summary and Prospects section.

Experimental Section

All ESR experiments were performed using the Cornell 2D spectrometer.[15,16] Details of sample preparation and experimental methodology are presented elsewhere.[30] The probes used were (a) C-P-P-P-P-A (monoradical) and (b) C-P-P-P-P-C

(biradical) dissolved in a glass-forming glycerol−water−trifluoroethanol solution. Here C, P, and A are cysteine, proline, and alanine, respectively, and the cysteines were labeled with the methanethiosulfonate spin label. 2D ESR (COSY and 2D ELDOR) experiments were performed in the slow motional regime at a range of temperatures from about −30 °C to −130 °C. At each temperature echo-2D ELDOR experiments were performed at about 8−10 values of the mixing times. The maximum mixing time at each temperature ranged from 2 to 60 μs. The experimental data was phase corrected, and the pure absorption line shapes were obtained using the procedure reported earlier.[30]

Theory for Pure Absorption Spectral Simulations

The dual-quadrature 2D ESR signal provides, in general, two types of coherence signals called $S_{c−}$ and S_{c+}.[22,30,34] In the slow motional regime these consist of complex Lorentzians with complex weighting factors. Due to substantial inhomogeneous broadening from large proton superhyperfine splittings and slow motions, the S_{c+} signal usually decays away in the instrumental dead-times. Additionally, the presence of these instrumental dead-times and also finite pulses results in large phase variations across the 2D frequency domain spectrum. Despite these challenges, the $S_{c−}$ signal in the slow motional regime can be phase corrected to obtain absorption-like spectra.[30]

To theoretically calculate the pure absorption 2D ESR spectra, we need to follow the evolution of the reduced density matrix, $\chi(\Omega,t) = \rho(\Omega,t) - \rho_0(\Omega)$, which is governed by the stochastic Liouville equation:[27,31]

$$\dot{\hat{\chi}}(\Omega,t) = i[\hat{H}(\Omega),\hat{\chi}(\Omega,t)] - \Gamma_\Omega \hat{\chi}(\Omega,t)$$

$$\equiv -\angle(\Omega)\,\hat{\chi}(\Omega,t) \tag{1}$$

where $H(\Omega)$ is the orientation-dependent spin Hamiltonian of the system, Γ_Ω is the time-independent diffusion superoperator, and $\angle(\Omega)$ is the stochastic Liouville operator. For 2D ESR spectral calculations this superoperator is diagonalized in each of the diagonal (zero-order coherence) and off-diagonal (± 1 coherences)[7,22] subspaces, i.e.

$$\mathbf{O_1}^{tr}\angle_1\mathbf{O_1} = \Lambda_1 \quad \mathbf{O_0}^{tr}\angle_0\mathbf{O_0} = \Lambda_0 \quad \mathbf{O_{-1}}^{tr}\angle_{-1}\mathbf{O_{-1}} = \Lambda_{-1} \tag{2}$$

where $\mathbf{O}$ is the complex symmetric matrix that diagonalizes $\angle(\Omega)$, and it consists of the eigenvectors, and Λ is the diagonal matrix consisting of the complex eigenvalues of the stochastic Liouville operator, and the subscripts refer to the order of the coherence. The real part of Λ provides the homogeneous line widths (i.e. $T_{2,j}^{-1}$), while the imaginary parts are the resonance frequency (f_j) of each "dynamic spin packet". The detailed properties of the Liouville operator are provided elsewhere.[7,22] In the absence of the nuclear Zeeman term

$$\mathbf{O_{-1}} = \mathbf{O_{+1}}^* \quad \text{and} \quad \Lambda_{-1} = \Lambda_{+1}^* \tag{3}$$

where the asterisk implies complex conjugation.

The time domain $S_{c−}$ 2D echo-ELDOR ESR signal can be written as[22,30]

$$S_{c-}(t_1,T_M,t_2) \propto \sum_{nmj} K_{nmj} \exp[-\{(\Lambda_{+1})_j + (\Lambda_{-1})_n\}t_1] \times$$
$$\exp[-(\Lambda_0)_m T_M] \exp[-(\Lambda_1)_n t_2] \exp(-\Delta t_2^2) \tag{4}$$

where the complex coupling coefficient, K_{nmj}, is given by

$$K_{nmj} =$$

$$\sum_{pkl} (\nu_{-1})_p (\mathbf{O_{-1}})_{pn} (\mathbf{O_{-1}})_{kn} (\mathbf{O_0})_{km} (\mathbf{O_0})_{lm} \sum_t (\mathbf{O_1})_{lj} (\mathbf{O_1})_{tj} (\nu_1)_t \quad (5)$$

Here $\nu_{\pm 1}$ are the two counter-rotating transition moment vectors that specify the transverse magnetization created by the first pulse, and $\Delta = 2\pi^2 \Delta_g^2$, where Δ_g is the inhomogeneous broadening assumed to be Gaussian. The phase variation due to the finite dead-times is corrected in the time domain, and the pure absorption 2D ESR line shapes are obtained by the following procedure[30]

$$S_{c-}^{abs}(f_1, T_M, f_2) = \mathcal{R}[\mathbf{FT_{t_2}}[\mathcal{R}\{\mathbf{FT_{t_1}}[S_{c-}(t_1, T_M, t_2)]\}]] \quad (6)$$

where $\mathbf{FT_{t_i}}$ ($i = 1, 2$) represent the complex Fourier transforms in t_1 and t_2 and $\mathcal{R}$ implies the extraction of the real part of the signal.

Note that the SECSY signal is the limit of the zero mixing time 2D echo-ELDOR signal, and hence it is given by the equivalent of eq 4 with $T_M = 0$. Also the COSY experiment (and an FID-based 2D ELDOR experiment) can be converted into the format of eq 4 by a shearing transform given by $t_2 \rightarrow t_2 + t_1$,[22,35] i.e.

$$S_{c-}^{SECSY}(t_1, t_2) \propto \sum_{nj} K_{nj} \exp[-\{(\Lambda_{+1})_j + (\Lambda_{-1})_n\} t_1] \times$$
$$\exp[-(\Lambda_1)_n t_2] \exp(-\Delta t_2^2) \quad (7)$$

with

$$K_{nj} = \sum_{pkt} (\nu_{-1})_p (\mathbf{O_{-1}})_{pn} (\mathbf{O_{-1}})_{kn} (\mathbf{O_1})_{kj} (\mathbf{O_1})_{tj} (\nu_1)_t \quad (8)$$

In eqs 4 and 7, the respective terms K_{nmj} and K_{nk} include the interference between the "dynamic spin packets". Also eq 7 is strictly valid for the limit of perfectly nonselective pulses.[22] For the case of FS-2D ESE the pulses are usually weak[18] (~ 1.1 G). As we have noted in the Introduction, this selective excitation curtails most of the interference between the "dynamic spin packets". This effect is, of course, not provided for in eq 7.

Millhauser and Freed[18] (MF) then assumed that in the near-rigid limit the elements of the complex orthogonal matrixes become nearly real. Thus from eq 3 $\mathbf{O_{-1}} = \mathbf{O_1}$. Using the properties of real orthogonal matrixes, we obtain from eq 8:[18]

$$K_{nj} = \delta_{nj} \sum_{pt} (\nu_{-1})_p (\mathbf{O_1})_{pn} (\mathbf{O_1})_{tn} (\nu_1)_t \quad (9)$$

Thus, the only terms surviving in eq 7 for the case of FS-2D ESE are those with $n = j$ (i.e. the diagonal terms). Hence this approximation, which we now know is not strictly valid, does serve the purpose of removing any interference between the "dynamic spin packets", which should be a good approximation for the FS-2D ESE experiment. In general, ν is imaginary. Then following MF[18] we write

$$K_{jj} \cong [\mathbf{O_1}^{tr} \nu_1]_j^2 \quad (10)$$

Next substituting eqs 9 and 10 into eq 7 and Fourier transforming it with respect to t_1 and t_2, MF obtained[18]

$$S^{FS2DESE}(f_1, f_2) \propto$$
$$\sum_j (\mathbf{O_1} \nu_1)_j^2 \frac{T_{2j}}{1 + f_1^2 T_{2j}^2} [e^{-2\tau_{1d} T_{2j}}] \exp[-(f_2 - f_j)^2 / \Delta^2] \quad (11)$$

where f_1 and f_2 are the two orthogonal frequency domains (i.e.

the Fourier transform variables with respect to t_1 and t_2, respectively). [In eq 11, τ_{2d}, the deadtime in t_2, has been set equal to τ_{1d} (the deadtime in t_1), reflecting the fact that, in the reported experiments, it is τ_{1d} (of 50 ns, compared to a τ_{2d} of 40 ns) that dictates the effective dead-time in an echo-based experiment.] Also, MF argue that this equation satisfies the set of inequalities given by

$$\gamma H_s > \Delta \omega_s \approx \Delta \gg \gamma H_1 \gg T_{2j}^{-1} \quad (12)$$

where H_s is the full width of the spectrum, $\Delta \omega_s$ is a measure of the width of spectral detail, and H_1 is the microwave field strength in the rotating frame.

Results and Discussion

We begin with the two-pulse COSY experiment. As mentioned above, a shearing transform[22,35] on the S_{c-} signal provides the SECSY experiment. Inhomogeneous broadening is refocused in this experiment, and hence one obtains the homogeneous line shapes in the f_1 domain, while the inhomogeneously broadened CW ESR-equivalent spectra occurs along the f_2 domain. The T_2 can be extracted by fitting a slice along f_1 of the absorption spectrum to a Lorentzian, i.e

$$y = \frac{cw}{w^2 + 4\pi^2 f_1^2} + b \quad (13)$$

where $T_2/2 = 1/w$, b is a baseline correction, and c the normalization constant. In Figure 1 we show the variation of T_2 as a function of temperature for the monoradical (Figure 1a) and the biradical (Figure 1b). These were obtained for two different values (-7 and 62 MHz) of f_2 corresponding to the maximum values of the two observable hf auto-peaks. The T_2's for the biradical are a little smaller than those of the monoradical, reflecting the extra contribution to relaxation from the modulation of the electron−electron dipolar interaction in the biradical. Also the variation in T_2 as a function of f_2 above -85 °C is thus clear (see also Figure 2a). The T_2's of the 62 MHz slice are consistently shorter than those of the -7 MHz slice. For temperatures above ca. -85 °C the T_2's increase as temperature decreases. This fact and the T_2 variation across the spectrum are consistent with the T_2's being dominated by the slow tumbling of the nitroxide in the glass above -85 °C. That is, this corresponds to the usual slow motional behavior.[6,17,18]

We fit the data above -85 °C for the monoradical to a function of the form $\ln(T_2) = \ln[(T_2)_0] + E_A/RT$ to obtain an average activation energy of $(5 \pm 0.9)/\alpha$ kcal/mol, where α is the parameter that depends upon the nature of the microscopic model for rotational diffusion as well as on the extent of inhomogeneous broadening[32] (cf. also the Introduction section). The T_2 variations of the experimental spectra fit well to a model of Brownian diffusion (cf. below) for which $\alpha \approx 0.5$,[7] thereby providing an activation energy of about 10 ± 1.8 kcal/mol.

However, at around -85 °C a new feature arises. The T_2's decrease as the temperature is lowered further. This was first observed by Stillman et al.[3] in a tempone in glycerol−water system, who ascribed it to a solid-state-like process. Later, Dzuba et al.[11] interpreted this feature as due to the thermally activated rotation of methyl groups in the nitroxide moiety, which modulates the electron−nuclear dipolar interaction with the methyl group protons. The contribution to T_2 from this process below 200 K led to a decrease in their two-pulse echo intensity as a function of temperature. A control experiment on a nitroxide which contains no methyl groups (Fremy's salt) in the same system did not lead to such a decrease,[11] verifying their conclusions. This process has recently been confirmed
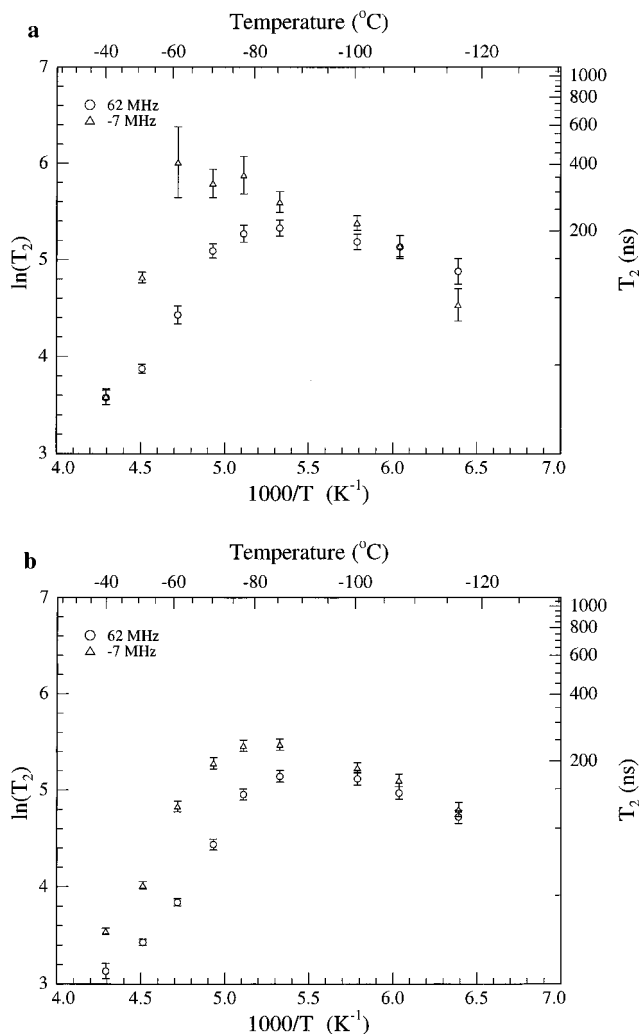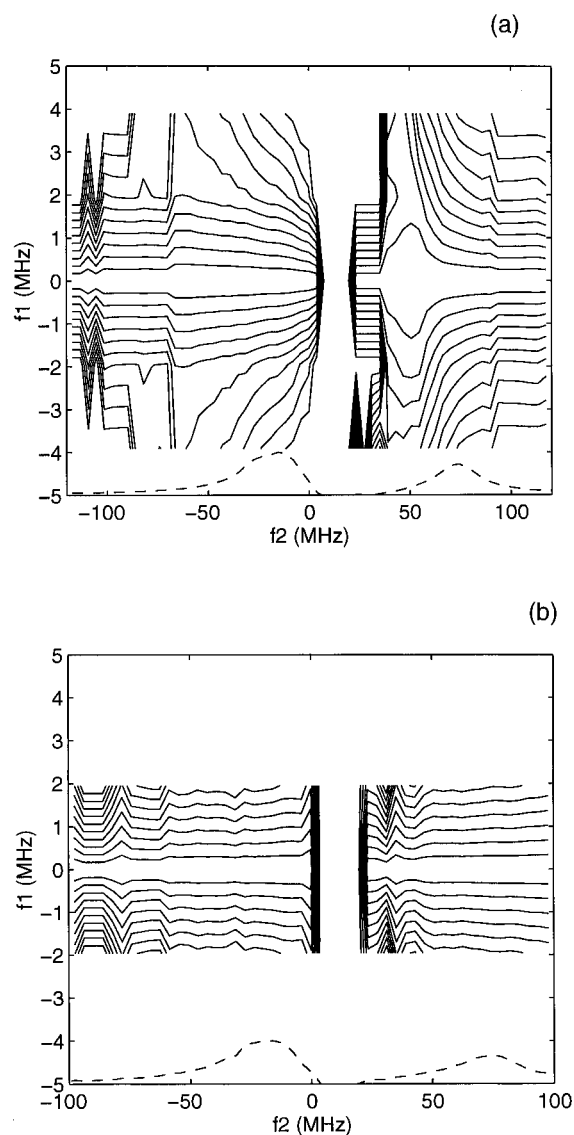
Figure 1. Variation of T_2 with temperature for the (a) monoradical and (b) biradical. Values shown are for the slices corresponding to the two maxima in f_2.

Figure 2. Normalized SECSY absorption contours for the monoradical at (a) −60 °C and (b) −105 °C. The $f_1 = 0$ MHz slices are shown by dashed lines.

by other workers for nitroxides in glass-forming matrixes (and in doped environments)[12] and in single crystals of γ-irradiated 4-methyl-2,6-di-*tert*-butylphenol.[13] The temperature dependence of the T_2 indicates that the internal motions of the methyl groups are in the fast motional regime.

Whereas the temperature dependence of the homogeneous line widths is instructive, the full power of SECSY absorption line shapes is conveyed by the normalized contours.[17,18] These are constructed from the experimental absorption data by taking a slice along f_1 for each value of f_2 and normalizing it so that the amplitude at $f_1 = 0$ is unity. The variation of intrinsic line widths as a function of f_2 becomes clear. This variation in line width is a key indicator of the mechanism of motional dynamics.[17,18]

The normalized contours for the monoradical are shown in Figure 2 at two temperatures. We find that above −85 °C there exists substantial variation in T_2 as a function of f_2, reflecting effects of the slow motions (cf. Figure 2a). However, below −85 °C the contours are flat, consistent with an orientation-independent T_2; that is, processes other than the slow overall reorientation dominate (cf. Figure 2b).

However, our SECSY experiments appear to have an instrumental artifact that led to a reduction of intensity between the observable hyperfine auto-peaks. We believe that this was due to the inadequate cancellation of baseline anomalies by the two-pulse sequence. This creates an artificial "zeroing" of the normalized contours (cf. Figure 2). 2D ELDOR with its 32-step phase cycling has been found to yield better baseline

cancellations than does COSY (or SECSY) with its 8-step phase cycling.[37] We note again that the zero mixing time 2D ELDOR experiment corresponds to the SECSY experiment. In this spirit, we have chosen to use the lowest mixing time 2D ELDOR experiment that we performed ($T = 100$ ns) at all temperatures as more reflective of the true variation in T_2.

For comparison with theory we performed a series of spectral simulations based on eqs 4 and 6 and the model of Brownian diffusion [which is characterized by the reorientational rates parallel ($R_{\parallel}$) and perpendicular ($R_{\perp}$) to a molecular defined diffusion axis; it is usual[22] to define an average rate ($\bar{R} = \sqrt[3]{R_{\parallel}R_{\perp}^2}$) and an anisotropy factor ($N = R_{\parallel}/R_{\perp}$)]. These are shown in Figure 3. The important variation of T_2 in these theoretical contours is conveyed by the innermost lines. The jagged outer contours relate to the spectral regions of low intensity and are relatively unimportant.

We find that the model of isotropic Brownian diffusion ($N = 1$) does not lead to line width variation across the spectrum (cf. Figure 3a−c) for the magnetic tensors used for this monoradical.[36] However the introduction of substantial anisotropy in the motion does create such a variation (cf. Figure 3d−f, where $N = 10$). We compare the −51 °C lowest mixing time ($T = 100$ ns) 2D ELDOR experiment with the theoretical

2D Electron Spin Resonance and Slow Motions

J. Phys. Chem. A, Vol. 101, No. 43, 1997 **8003**
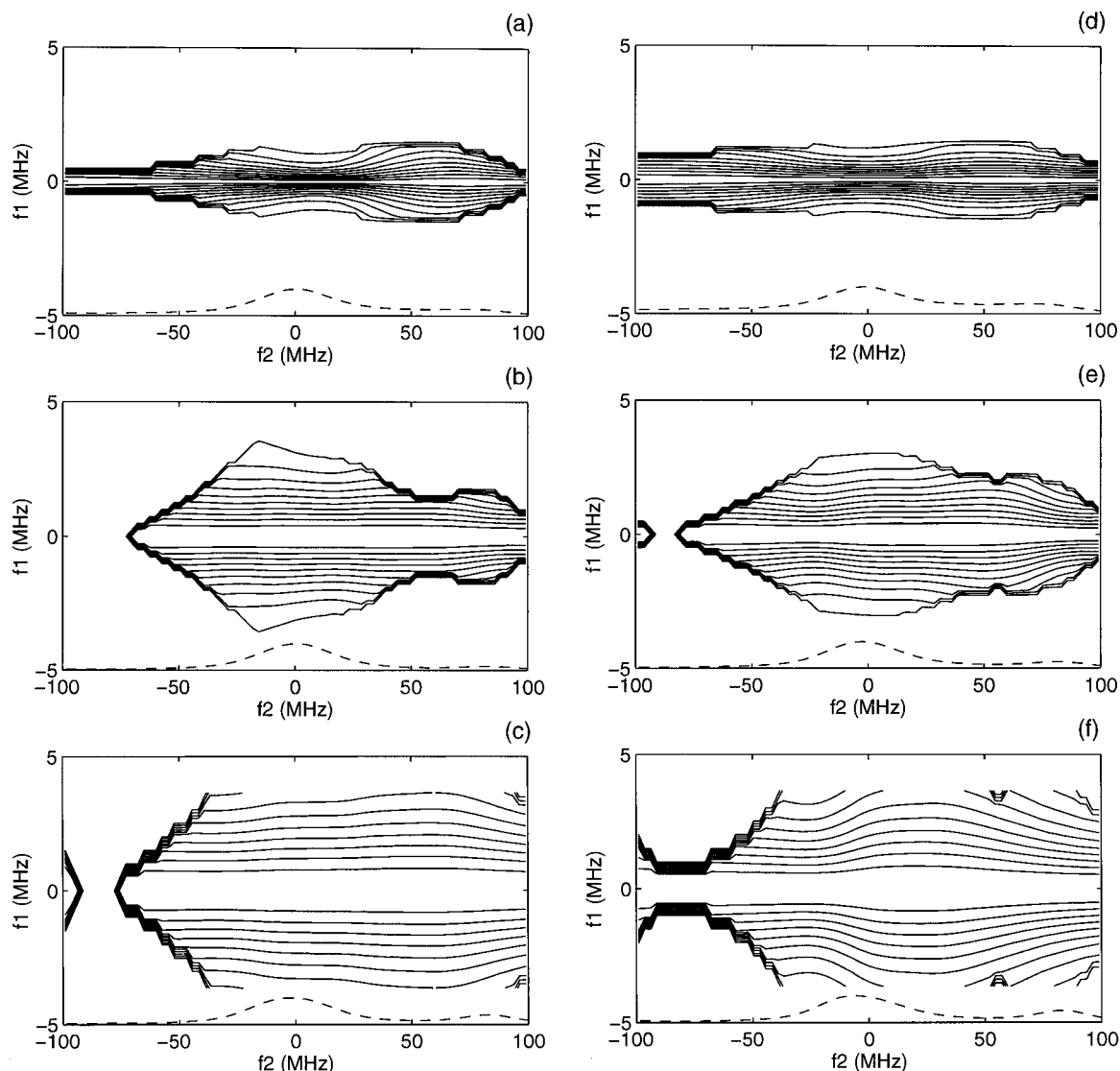
Figure 3. Theoretical normalized contours at different motional rates for the model of Brownian diffusion. (a) $\bar{R} = 2 \times 10^3$ s^{-1}, $N = 1$; (b) $\bar{R} = 2 \times 10^4$ s^{-1}, $N = 1$; (c) $\bar{R} = 1.58 \times 10^5$ s^{-1}, $N = 1$; (d) $\bar{R} = 2 \times 10^3$ s^{-1}, $N = 10$; (e) $\bar{R} = 2 \times 10^4$ s^{-1}, $N = 10$; and (f) $\bar{R} = 1.58 \times 10^5$ s^{-1}, $N = 10$. $\bar{R}$ is defined in the text. The magnetic parameters were $g_{xx} = 2.0089$, $g_{yy} = 2.0058$, $g_{zz} = 2.0022$, $A_{xx} = 5.27$, $A_{yy} = 5.27$, $A_{zz} = 36.0$. Other simulation parameters were $\Delta_G = 2.0$ G, $B_0 = 3200$ G. The dead times in t_1 and t_2 were 50 ns. The pruned basis set (3% pruning tolerance) consisted of a minimum truncation set of $L_{max}^e = 92$, $L_{max}^o = 41$, $K_{max} = 26$, and $M_{max} = 2$.

contours in Figure 4. The variation in line widths as a function of f_2 is similar, indicating a model of anisotropic Brownian diffusion, characterized by a large N (which was set equal to 100 in Figure 4b) and $\bar{R} = 1 \times 10^6$ s^{-1} (i.e. $\tau_R = 1/6\bar{R} = 0.17$ μs). Note that due to the large computational effort involved in simulating such slow motional spectra,[22] we did not attempt to optimize the value of N. However, our results show that a model of *very* anisotropic Brownian diffusion is required to theoretically reproduce the experimental normalized contours. The theoretical normalized contours for N of 100 and $\bar{R} = 2 \times 10^3$ s^{-1} (i.e. $\tau_R = 83$ μs) showed no variation across the spectrum, and these correspond to the experimental data at -85 °C.

We note that this result is in contradiction to the earlier results of Millhauser and Freed,[18] who found that isotropic ($N = 1$) Brownian diffusion would lead to large variation in T_2. Also, they observed from their simulations that such variations occur even at a very low rotational rate ($\bar{R} = 5 \times 10^3$ s^{-1}). However, they used a simplifying assumption in their theoretical analysis, that the eigenvectors of the SLE are real in the slow motional regime (cf. the Theory section). This removed the interference between the "dynamic spin packets" and led to the form of eq 11 for their experiment.

We find that using eq 11 and taking $\mathcal{R}$ $[(\mathbf{O_1}\nu)_j]^2$ does qualitatively replicate their results (cf. Figure 5), and we note that the selectivity of the irradiation in their FS-2D ESE experiment should greatly reduce any interferences between "dynamic spin packets". Hence their assumptions leading to eq 11 should provide a closer approximation to their experiment than forms based on eq 7. The correct verification of this phenomenon would require exact numerical simulations that include the finiteness of the pulse. Note that the contours are quite sensitive to the precise values of the g and hf terms that are used,[18b] and improved computational techniques now lead to better convergence of the spectra.

In fact, small changes in the magnetic tensors strongly affect the detailed T_2 variations across the spectrum for the case of isotropic reorientation.[18b] Millhauser and Freed[18b] attributed this to certain accidental degeneracies of the parallel edge in the central region of the spectrum. Thus for the case of SECSY, the use of magnetic parameters ($g_{xx} = 2.0096$, $g_{yy} = 2.0063$, $g_{zz} = 2.0022$, and $A_{xx} = 6.5$, $A_{yy} = 4.5$, and $A_{zz} = 33.4$) did provide a T_2 variation across the spectrum for $\bar{R} = 1 \times 10^4$ s^{-1} and $N = 1$ (cf. Figure 6b). However it is again true that simulations

(a)

(b)
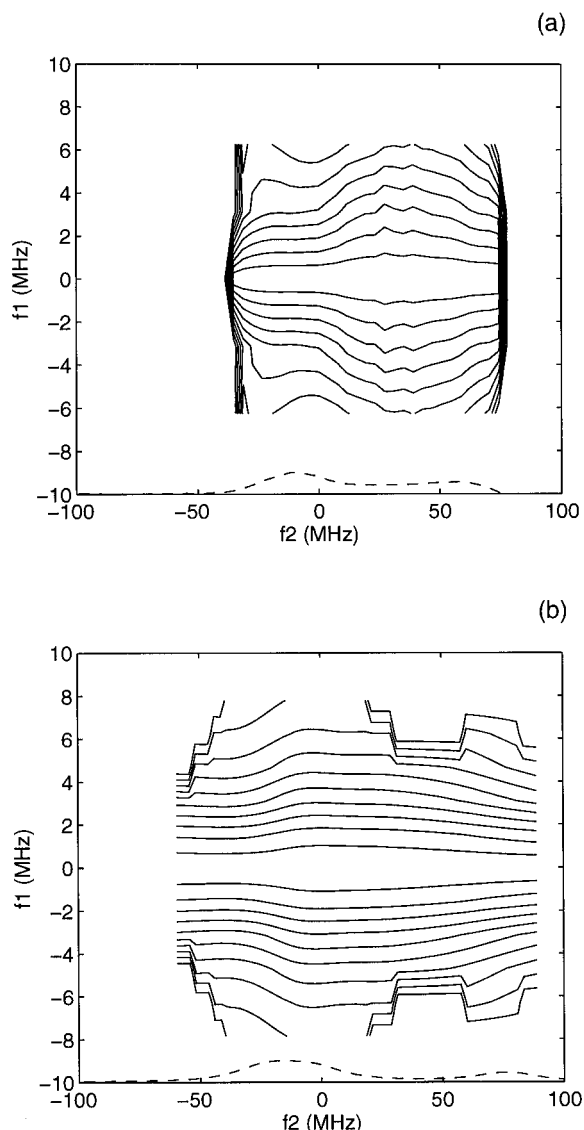
Figure 4. Comparison of (a) experimental absorption 2D ELDOR (T = 100 ns) spectrum at -51 °C for the monoradical with (b) theory. Normalized contours are shown. The theoretical parameters were $\bar{R} = 1 \times 10^6$ s^{-1}, $N = 100$. The magnetic parameters were $g_{xx} = 2.00839$, $g_{yy} = 2.00612$, $g_{zz} = 2.00228$, $A_{xx} = 7.5$, $A_{yy} = 5.7$, $A_{zz} = 37.3$. The magnetic tensors were obtained by simulating a 250 GHz rigid limit spectrum. Other simulation parameters were $\Delta_G = 2.0$ G, $B_0 = 3361$ G. The dead times in t_1 and t_2 were 50 ns. The pruned basis set (1% pruning tolerance) consisted of a minimum truncation set of $L^e_{max} = 80$, $L^o_{max} = 51$, $K_{max} = 24$, and $M_{max} = 2$.

for the FS-2D ESE line shapes using eq 11 show a more pronounced T_2 variation than the SECSY simulation (cf. Figure 6b).

The FS-2D ESE experiment, then, contains inherent advantages for measuring slower dynamics and resolving mechanisms of dynamics as compared to the SECSY experiment. However, it is limited to longer T_2's, and it requires much longer acquisition times, as we have noted in the Introduction.

We now turn to the 2D ELDOR experiment. Some representative pure absorption spectra are shown in Figure 7. As the motion slows down, the high-frequency hf peak shows a splitting (cf. Figure 7, parts b, c vs a). However, this feature disappears rapidly with mixing time (cf. Figure 7, parts e, f vs b, c). We note that this effect, hitherto unobserved experimentally, could arise from the modulation due to proton–electron interactions, as has been postulated theoretically[34] for frozen samples. At -51 °C, inhomogeneous contributions to the line widths due to slow tumbling of the molecule might serve to


(a)

(b)

(c)
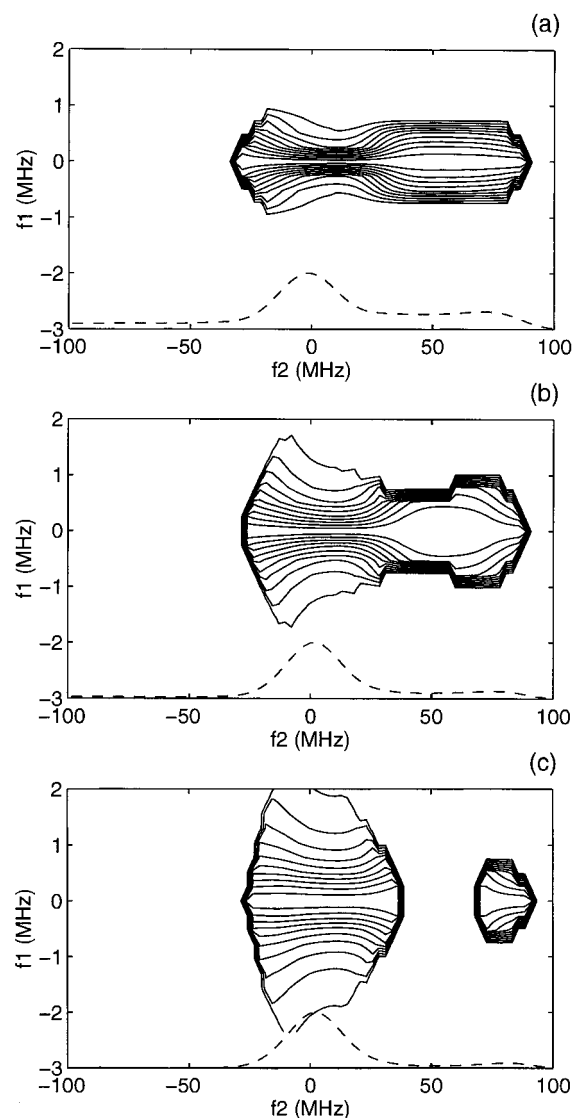
Figure 5. Theoretical normalized contours for the model of Brownian diffusion obtained using the assumptions of Millhauser and Freed.[18] (a) $\bar{R} = 2 \times 10^3$ s^{-1}, $N = 1$; (b) $\bar{R} = 5 \times 10^3$ s^{-1}, $N = 1$; and (c) $\bar{R} = 1 \times 10^4$ s^{-1}, $N = 1$. The dead times in t_1 and t_2 were 200 *ns* and $\Delta_G = 2.0$ G. The magnetic and minimum truncation set parameters were the same as Figure 3.

mask these modulation peaks. This observation demonstrates the need for 2D experiments at small mixing times (i.e. 0–100 ns), even in cases where the dynamic effects occur over a much longer time scale (i.e. μs). Another potential source of modulation is one that applies to the biradical, viz. an unrefocused modulation along $t_1 = t_2$ in the SECSY experiment due to the dipolar interaction between the two electron spins, sometimes called "instantaneous diffusion".[38,39]

In the 2D ELDOR experiment, cross peaks can form due to magnetization transfer during the mixing time. However these experiments were marked by the absence of first- and second-order cross-peaks which arise from the intramolecular ^{14}N electron–nuclear dipolar (END) and the intermolecular Heisenberg spin exchange (HE) interactions (and/or electron–electron dipolar interactions, EED). Note that in such a viscous environment and at these concentrations of spins (1 mM) the contributions of the concentration-dependent interactions (i.e. HE and EED) are expected to be very small. The absence of these cross-peaks also indicates that any rotationally invariant nuclear spin–lattice relaxation[26,27] is small.

Why is the END interaction "ineffective" in creating substantial single- and double-order cross-peaks in the experiment?

2D Electron Spin Resonance and Slow Motions

J. Phys. Chem. A, Vol. 101, No. 43, 1997 **8005**

(a)

(b)
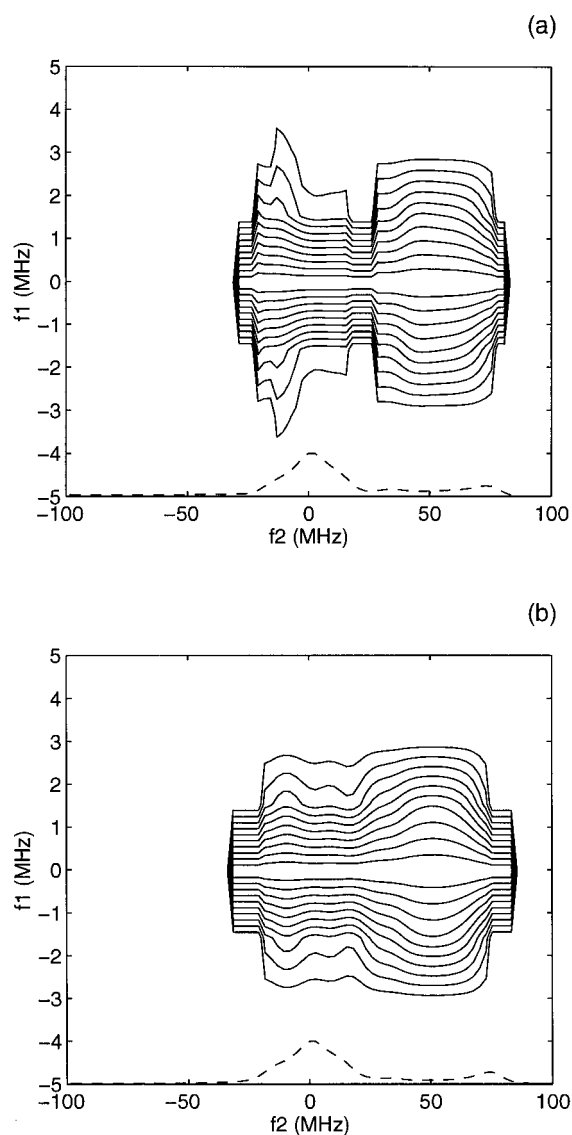
Figure 6. Theoretical normalized contours for the model of Brownian diffusion for the (a) SECSY and (b) FS-2D ESE experiments. The simulation parameters were $\bar{R} = 1 \times 10^4$ s^{-1}, $N = 1$. The dead times in t_1 and t_2 were 50 ns and $\Delta_G = 2.0$ G. The magnetic parameters were $g_{xx} = 2.0096$, $g_{yy} = 2.0063$, $g_{zz} = 2.0022$, $A_{xx} = 6.5$, $A_{yy} = 4.5$, $A_{zz} = 33.4$. The pruned basis set (3% pruning tolerance) consisted of a minimum truncation set of $L_{max}^e = 72$, $L_{max}^o = 31$, $K_{max} = 28$, and $M_{max} = 2$.

To understand this, we performed a number of theoretical simulations, wherein the contribution to cross-peak growth from this effect is "naturally" included.[22] In Figure 8 we show three simulations for different rotational rates based on the model of very anisotropic Brownian motion for a mixing time, T_M, of 64 μs. Anisotropic motion is appropriate for an end-labeled macromolecule.[40] Cross-peak formation due to the rotation-induced modulation of the END interaction is negligible for $\bar{R} = 1 \times 10^4$ s^{-1} (which corresponds to the experimental spectrum at about -85 °C), and is very small for motional rates in the range 1×10^5 to 1×10^6 s^{-1}. The latter corresponds to the experiments at -51 °C (cf. above). Experimentally, these cross-peaks would be attenuated due to the imperfect coverage of our finite pulses (the coverage at ± 100 MHz was about 80% of that at the center). Also, the theoretical signal intensity for the 1×10^6 s^{-1} case is 2 orders of magnitude smaller than that for the case of 1×10^4 s^{-1}, providing by itself a huge challenge for experimentally observing these spectra, let alone the weak cross-peaks. Note that at -51 °C ($\bar{R} = 1 \times 10^6$ s^{-1}, $N = 100$,

cf. above) the maximum mixing time that would still yield a reasonable 2D S/N experimentally was 3 μs.

Another effect that can reduce cross-peaks is the so-called MOMD effect.[22,40] It stands for microscopic order with macroscopic disorder, and it has been applied to an analysis of an end-chain-labeled polymer liquid-crystal in the solid state.[40]

On the other hand, the auto-peaks themselves become broader with increased mixing time due to the growth of SD cross-peaks (cf. Introduction section). This increase in apparent line widths, which we call the "apparent T_2^{-1}", is shown in Figure 9 at four representative temperatures for the monoradical slices corresponding to the two maxima along f_2, of the hf auto-peaks.

To distinguish between contributions from the different SD mechanisms (cf. Introduction section) that lead to such cross-peak development, an estimate of the order of the effect and also its correlation times is helpful. We find we can obtain such an estimate by modeling the results of Figure 9 by an empirical equation of the form

$$T_2^{-1}(T_M) - T_2^{-1}(0) = \delta[1 - \exp(-T_M/\tau_c)] \qquad (14)$$

where $T_2(T_M)$ is the "apparent T_2" for a mixing time, T_M, $T_2(0)$ is the T_2 obtained from a SECSY experiment, δ represents the magnitude of the effect, and τ_c is the correlation time. The variation of δ and τ_c as a function of temperature is plotted in Figures 10 and 11 for the monoradical at the two spectral maxima in f_2.

We discuss first the magnitude of the effect, δ, which is plotted in Figure 10. The data above -60 °C could not be accurately fit to the form of eq 14, as is evident from the large errors in δ above this temperature (cf. Figure 10). This was, in part, due to our inability to measure the limiting value of the auto-peak width due to the rapid decay of the signal as a function of mixing time. The value of δ, between -60 and -85 °C, is constant within experimental error (about 1.8 and 1.4 G for the -7 and 62 MHz slices, respectively). The values above -85 °C are lower (i.e. below 1.5 G), and a trend is less evident. The correlation times increase as temperature decreases until about -85 °C. However, below -85 °C the correlation times become shorter as temperature is decreased further.

We would now like to examine our 2D ELDOR results for the temperature region above -85 °C. On the basis of our COSY results, we would surmise that the dominant mechanism for the generation of cross-peaks in this regime would be "rotational cross peaks" induced by slow tumbling.

We find that the growth of SD cross-peaks from theoretical simulations based on the model of Brownian diffusion does fit very well to the form of eq 14. The values of τ_c and δ obtained from these simulations (for the central auto-peak, i.e. corresponding to the experimental -7 MHz slice) are provided in Table 1. The values of τ_c obtained from simulations correspond well to those obtained experimentally. For example, for the case of (a) $\bar{R} = 1 \times 10^6$ s^{-1} and $N = 100$, the theoretical value of 3 μs corresponds well to the experimental value at -51 °C (cf. Figure 11) of 2.6 μs, and for (b) $\bar{R} = 1 \times 10^4$ s^{-1} and $N = 100$, the theoretical value of 23 μs corresponds to the experimental value at -77 °C of 28 μs. The values of δ obtained from the theoretical simulations demonstrate that these "reorientational cross-peaks" can, in fact, provide a broadening in the range 0.8–2.0 G (cf. Table 1). Therefore, we conclude that above -85 °C the slow reorientation of the molecule constitutes the primary source for SD cross-peaks. However, the theoretical simulations (cf. Table 1) indicate that the value of δ should depend more on τ_R.

We now turn to the temperature region below -85 °C, where the T_2's were dominated by the fast internal rotations of the methyl groups in the nitroxide moiety (cf. above), and the overall
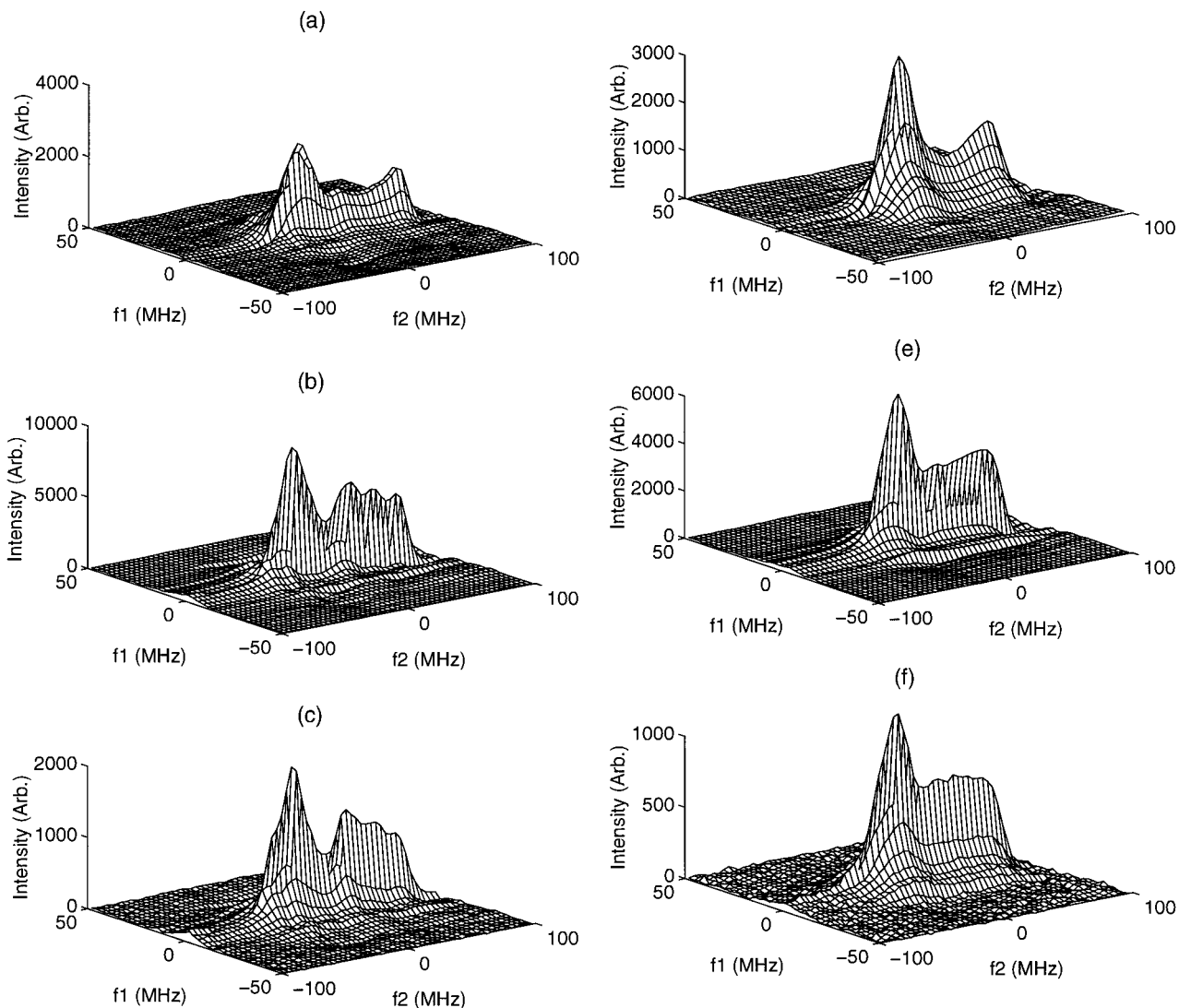
Figure 7. Experimental 2D ELDOR absorption spectra for the monoradical. Spectra shown are for (a) $T = -51$ °C, $T_M = 100$ ns; (b) $T = -77$ °C, $T_M = 100$ ns; (c) $T = -116$ °C, $T_M = 100$ ns; (d) $T = -51$ °C, $T_M = 200$ ns; (e) $T = -77$ °C, $T_M = 1000$ ns; and (f) $T = -116$ °C, $T_M = 1000$ ns.

reorientational motion of the nitroxide was too slow to exhibit any T_2 variation. While very slow tumbling of the probe can lead to SD cross-peak formation without providing any T_2 variation (cf. Introduction section), this mechanism is inconsistent with the observation that the correlation time for the process is decreasing with decreasing temperature, since it naturally yields *increasing* correlation times with decrease in temperature. An additional source of SD broadening would be due to the methyl proton END interaction with the electron spin. In the limit of rapid methyl group internal rotations it would again require the slow overall tumbling to provide SD. This would be an unsatisfactory explanation for the same reason as that for averaging the ^{14}N hf tensor and the g tensor and will mainly provide a small additional contribution to these dominant terms.[13,43]

However, the methyl group internal rotations can, as they slow down, lead to nuclear spin-flips, which will cause SD between the different unresolved shf lines of the methyl protons. Such spin-flip rates, W_n, may be estimated from standard expressions,[42] i.e.

$$W_n = \frac{1}{60}[\Delta A^H(\Omega)]^2 \frac{\tau_I}{1 + \omega_a^2 \tau_I^2} \tag{15}$$

where τ_I is the correlation time for internal motion, and ω_a is

approximately the proton Larmor frequency ($\sim 8.8 \times 10^7$ s^{-1}). Also $\Delta A^H(\Omega)$ represents that portion of the methyl proton hf tensor that is averaged by the internal rotations, and it depends on the overall molecular orientation, Ω. It can be estimated from literature data on the proton–electron dipolar interaction[41] in nitroxides. We used a value of 1 G. For 12 equivalent methyl protons a simple analysis shows that the effective spin-flip rate is about $5W_n$.

Using eq 15 we find that with a τ_I of 10^{-9} s we estimate $5W_n = 2.5 \times 10^4$ s^{-1}, which is in reasonable agreement with the experimental value of $1/\tau_c \approx 3.3 \times 10^4$ s^{-1} at -85 °C. With a τ_I of 10^{-8} s we obtain a spin-flip rate $5W_n = 6.5 \times 10^{-5}$ s^{-1}, which corresponds well to the experimental estimate of $1/\tau_c \approx 1.4 \times 10^5$ s^{-1} at -116 °C. Thus this mechanism has the correct temperature dependence. While these estimates of the spin-flip rates are hardly quantitative, because of the simplicity of our analysis, they do indicate that this mechanism could account for the observed SD below -85 °C. Besides, in this regime (corresponding to a τ_I of ca. $10^{-8}-10^{-9}$ s) the methyl group rotations would still be in the fast motional regime, so that they would lead to a decrease in T_2 with a decrease in temperature, as we observed in our COSY experiments.[43]

It would be premature to ascribe the SD cross-peak formation below -85 °C to be due to the fast internal rotations of the methyl groups. An important experiment would be the use of

2D Electron Spin Resonance and Slow Motions

J. Phys. Chem. A, Vol. 101, No. 43, 1997 **8007**
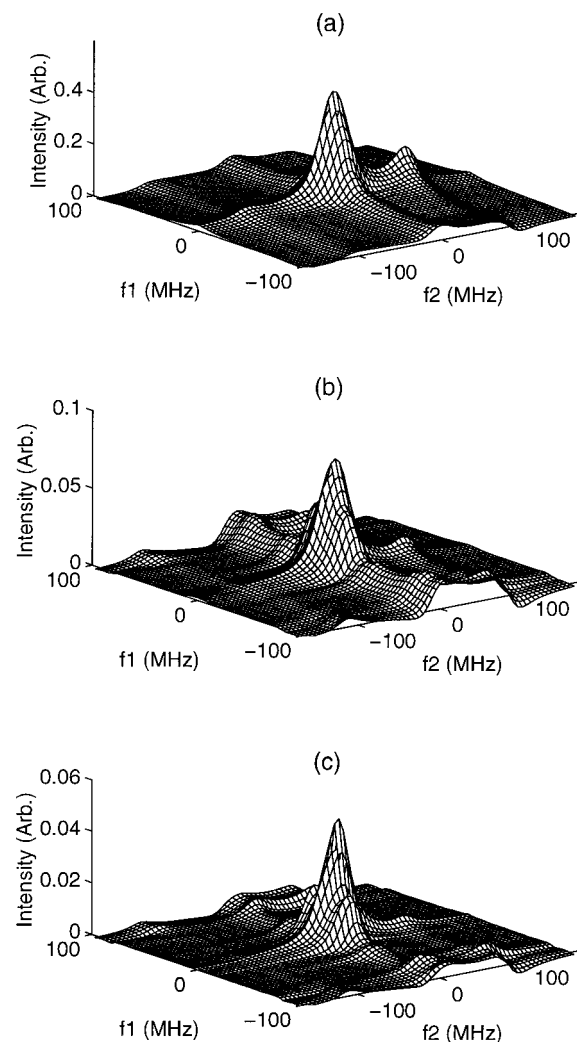
Figure 8. Theoretical absorption 2D ELDOR spectra for mixing time, T_M, of 64 μs, with $N = 100$ and rotational rate, $\bar{R}$, of (a) 1×10^4 s^{-1}, (b) 1×10^5 s^{-1}, and (c) 1×10^6 s^{-1}. The magnetic parameters were $g_{xx} = 2.0086$, $g_{yy} = 2.0064$, $g_{zz} = 2.0032$, $A_{xx} = 6.23$, $A_{yy} = 6.23$, $A_{zz} = 35.7$. Other simulation parameters were $\Delta_G = 2.0$ G, $B_0 = 3361$ G. The dead times in t_1 and t_2 were 50 ns. The pruned basis set (3% pruning tolerance) consisted of a minimum truncation set of $L_{max}^e = 78$, $L_{max}^o = 17$, $K_{max} = 18$, and $M_{max} = 2$.

probes with deuterated methyl groups to eliminate the contribution of the methyl protons to both the T_2 as well as to SD. Finally, we note that the mechanism of spin diffusion via the bath of protons in the solvent,[21,23] which can create SD cross-peaks, has not been explored.

Summary and Prospects

2D ELDOR experiments in the slow motional regime on a nitroxide spin label in a glass-forming medium have been reported. The experimental T_2's above -85 °C are dominated by the slow tumbling of the probe. A decrease in T_2 as the temperature is decreased below -85 °C is ascribed to the rapid modulation of the dipolar interaction between the methyl proton in the nitroxide moiety and the electron spin, in light of earlier works.[11-13] The use of pure absorption spectra[30] allows the variation of T_2 across the spectrum to be monitored. It is shown that the model of anisotropic Brownian diffusion provides semiquantitative agreement with such a variation, but the effects of MOMD have yet to be explored.

The absence of first- and second-order cross-peaks in the 2D ELDOR experiments is rationalized in terms of the following: primarily the very slow tumbling of the molecules leading to
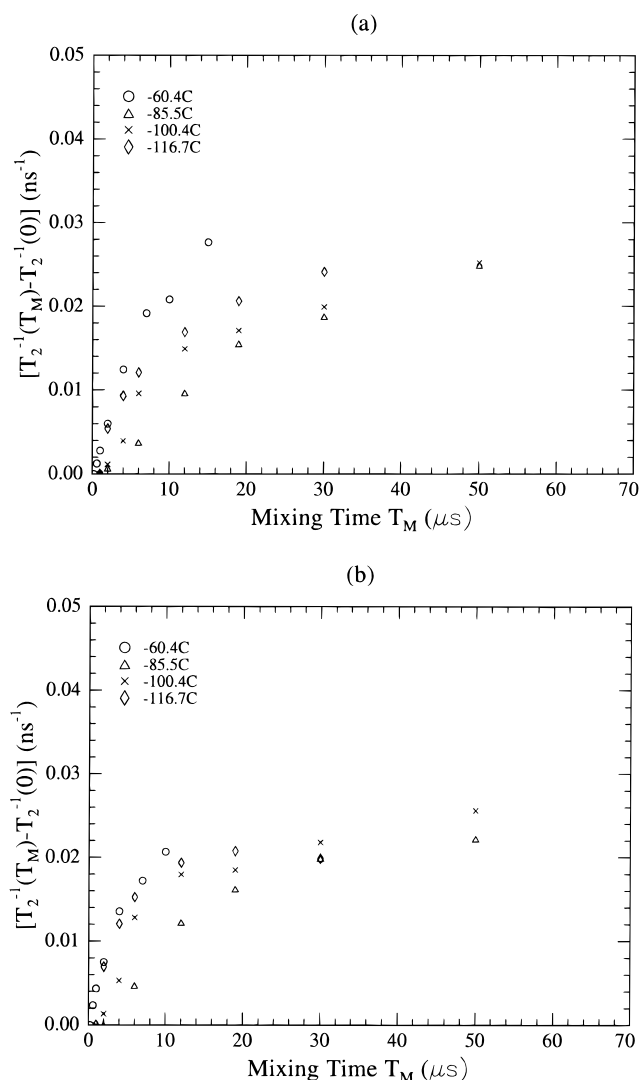

Figure 9. Growth of SD cross-peaks during the mixing time for the monoradical. Values shown are for the two slices corresponding to the maximum in f_2 of the hf auto-peaks. Figures shown correspond to the slice at (a) -7 and (b) 62 MHz.
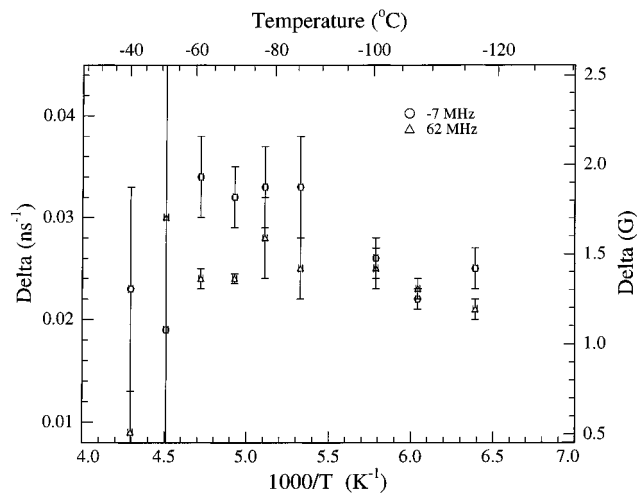
Figure 10. Variation of δ with temperature. Values shown are for the slices corresponding to the two maxima in f_2, at -7 and 62 MHz.

only small cross-peaks in the theoretical predictions, but also to some attenuation of these cross-peaks due to imperfect coverage in the experiment, and possibly the effects of MOMD.

The rate of growth of SD cross-peaks above -85 °C has been shown to arise principally from spectral diffusion associated with the slow reorientation of the molecule modulating the ^{14}N
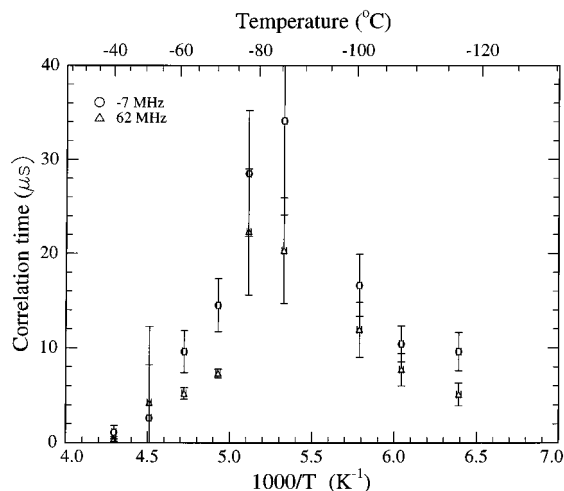
Figure 11. Variation of τ_c with temperature. Values shown are for the slices corresponding to the two maxima in f_2, at -7 and 62 MHz.

TABLE 1: δ and τ_c Obtained from Theoretical Simulations

R (s^{-1})	N	δ (ns^{-1})	τ_c (μs)
1×10^4	100	0.028 ± 0.007	23 ± 5
1×10^4	1	0.036 ± 0.002	17 ± 2
1×10^5	100	0.031 ± 0.002	11 ± 2
1×10^5	1	0.034 ± 0.003	4 ± 1
1×10^6	100	0.015 ± 0.003	3 ± 2

END and *g*-tensor interactions. This process can be used to study the motional dynamics. A method is shown for extracting a correlation time, τ_c, by monitoring the growth of these SD cross-peaks. This procedure is verified theoretically, and good agreement between experiment and theory is obtained. We note that theoretical simulations can be performed as a function of τ_R, and the growth of SD cross-peaks (from the reorientational dynamics) can be used to relate the τ_c obtained from these simulations to τ_R, in analogy to earlier examples.[3,22,32] This would lead to a relatively simple procedure for using 2D ESR to directly determine the rotational correlation time, short of detailed simulations.

The anomalous temperature dependence of the experimental τ_c below -85 °C cannot be explained either by (a) slow reorientation of the probe leading to a modulation of the ^{14}N END and *g* tensor interactions or by (b) spin-flips of the methyl protons on the nitroxide moiety due to rotational modulation of the electron−proton hf tensor by the same slow overall rotation of the spin-labeled molecule. However, such spin-flips due to the more rapid internal rotations of the methyl groups on the nitroxide moiety could possibly explain these experimental results. Further experiments are required to confirm this.

References and Notes

(1) Brown, I. M. *J. Chem. Phys.* **1974**, *60*, 4930.
(2) Schwartz, R. N.; Jones, L. L.; Bowman, M. K. *J. Phys. Chem.* **1979**, *84*, 3429.
(3) A. E. Stillman, A. E.; Schwartz, L. J.; Freed, J. H. *J. Chem. Phys.* **1980**, *73*, 3502; **1982**, *76*, 5658.
(4) Freed, J. H. *Spin Labeling: Theory and Application*; Berliner, L. J., Ed.; Academic: New York, 1976; Vol 1, Chapter 3.
(5) Stillman, A. E.; Schwartz, R. N. *Time Domain Electron Spin Resonance*; Kevan, L., Schwartz, R. N., Eds.; Wiley: New York, 1979; Chapter 5.
(6) Schwartz, L. J.; Stillman, A. E.; Freed, J. H. *J. Chem. Phys.* **1982**, *77*, 5410.
(7) Schwartz, L. J. Ph.D. Thesis, Cornell University, 1986.
(8) Hwang, J. S.; Mason, R. P.; Hwang, L. P.; Freed, J. H. *J. Phys. Chem.* **1975**, *79*, 489.

(9) Budker, V.; Du, J. L.; Seiter, M.; Eaton, G. R.; Eaton, S. S. *Biophys. J.* **1995**, *68*, 2531.
(10) Rakowsky, M. H.; More, K. M.; Kulikov, A.; Eaton, G. R.; Eaton, S. S. *J. Am. Chem. Soc.* **1995**, *117*, 2049.
(11) Dzuba, S. A.; Maryasov, A. G.; Salikhov, K. M.; Tsvetkov, Yu. D. *J. Magn. Reson.* **1984**, *58*, 95.
(12) Eaton, S. S.; Eaton, G. R. *Curr. Top. Biophys.* **1996**, *20*, 9, and references therein.
(13) Brustolon, M.; Maniero, A. L.; Bonora, M.; Segre, U. *Appl. Magn. Reson.* **1996**, *11*, 99.
(14) Luckhurst, G. R. *Spin Labeling: Theory and Application*; Berliner, L. J., Ed.; Academic: New York, 1976; Vol 1, Chapter 4.
(15) Gorcester, J.; Freed, J. H. *J. Chem. Phys.* **1986**, *85*, 5375.
(16) Gorcester, J.; Freed, J. H. *J. Chem. Phys.* **1988**, *88*, 4678.
(17) Gorcester, J.; Millhauser, G. L.; Freed, J. H. *Modern Pulsed and Continuous Wave Electron Spin Resonance*; Kevan, L., Bowman, M. K., Eds.; Wiley: New York, 1990; Chapter 3.
(18) Millhauser, G. L.; Freed, J. H. *J. Chem. Phys.* **1984**, *81*, 37. (b) Millhauser, G. L.; Freed, J. H. *J. Chem. Phys.*, **1986**, *85*, 63.
(19) Dzuba, S. A.; Tsvetkov, Yu. D. *Chem. Phys. Lett.* **1992**, *188*, 217.
(20) Salikhov, K. M.; Schneider, D. J.; Saxena, S.; Freed, J. H. *Chem. Phys. Lett.* **1996**, *262*, 17.
(21) Lee, S.; Patyal, B. R.; Freed, J. H. *J. Chem. Phys.* **1993**, *98*, 3665.
(22) Lee, S.; Budil, D. E.; Freed, J. H. *J. Chem. Phys.* **1994**, *101*, 5529.
(23) Salikhov, K. M.; Tsvetkov, Yu. D. *Time Domain Electron Spin Resonance*; Kevan, L., Schwartz, R. N., Eds.; Wiley: New York, 1979; Chapter 7.
(24) Dzuba, S. A.; Tsvetkov, Yu. D. *Chem. Phys.* **1988**, *120*, 291.
(25) Hornak, J.; Freed, J. H. *Chem. Phys. Lett.* **1983**, *101*, 115.
(26) Schwartz, L. J.; Millhauser, G. L.; Freed, J. H. *Chem. Phys. Lett.* **1986**, *127*, 60.
(27) Schneider, D. J.; Freed, J. H. *Advances in Chemical Physics, Vol. LXIII*; Hirschfelder, J. O., Wyatt, R. E., Coalson, R. D., Eds.; Wiley: New York, 1989; Chapter 10.
(28) (a) Patyal, B. R.; Crepeau, R. H.; Gamliel, D.; Freed, J. H. *Chem. Phys. Lett.* **1990**, *175*, 445. (b) Patyal, B. R.; Crepeau, R. H.; Gamliel, D.; Freed, J. H. *Chem. Phys. Lett.* **1990**, *175*, 453.
(29) (a) Robinson, B. H.; Haas, D. A.; Mailer, C. *Science* **1994**, *263*, 490. (b) Haas, D. A.; Mailer, C.; Robinson, B. H. *Biophys. J.* **1993**, *64*, 594.
(30) Saxena, S.; Freed, J. H. *J. Magn. Reson.* **1997**, *124*, 439.
(31) Freed, J. H.; Bruno, G. V.; Polnaszek, C. F. *J. Phys. Chem.* **1971**, *75*, 3385.
(32) Mason, R. P.; Freed, J. H. *J. Phys. Chem.* **1974**, *78*, 1321.
(33) Saxena, S.; Freed, J. H. *Chem. Phys. Lett.* **1996**, *251*, 102.
(34) Gamliel, D.; Freed, J. H. *J. Magn. Reson.* **1990**, *89*, 60.
(35) Ernst, R. R.; Bodenhausen, G.; Wokaun, A. *Principles of Nuclear Magnetic Resonance in One and Two Dimensions*; Clarendon: Oxford, 1987.
(36) Miick, S. M.; Millhauser, G. L. *Biophys. J.* **1992**, *63*, 917.
(37) Borbat, P.; Crepeau, R. H.; Freed, J. H. *J. Magn. Reson.* **1997**, *127*, 155.
(38) (a) Dikanov, S. A.; Tsvetkov, Yu. D. *Electron Spin Echo Envelope Modulation (ESEEM) Spectroscopy*; Chemical Rubber: Boca Raton, 1992. (b) Salikhov, K. M.; Dzuba, S. A.; Raitsimring, A. M. *J. Magn. Reson.* **1981**, *42*, 255.
(39) In actual fact we do not observe any such modulation effect for the dipolar interaction of 2.3 G in the SECSY experiment,[33] and furthermore rigorous rigid limit simulations [Saxena, S.; Freed, J. H. *J. Chem. Phys.* **1997**, *107*, 1317] do not lead to any observable differences in the predicted SECSY of the biradical vs the monoradical arising from this static interaction. It is well-known that the manifestation of these dipolar interactions in the spin−echo decay is suppressed by (1) the averaging over all orientations in a glass; by (2) the fact that with incomplete spectral coverage by our microwave pulses the two nitroxide electron spins (which typically resonate at different frequencies) will be rotated to a different extent by the finite pulses; and also by (3) the fact that the details of modulation, even for perfectly selective pulses, depend on the differences between the local fields sensed by each electron spin, due to the effects of their respective *g* and hf tensors.[38]
(40) Xu, D.; Crepeau, R. H.; Ober, C. K. Freed, J. H. *J. Phys. Chem.* **1996**, *100*, 15873.
(41) Brustolon, M.; Maniero, A. L.; Ottaviani, M. F.; Romanelli, M.; Segre, U. *J. Phys. Chem.* **1990**, *94*, 6589.
(42) Budil, D. E.; Earle, K. A.; Freed, J. H. *J. Phys. Chem.* **1993**, *97*, 1294.
(43) An estimate of W_n from the appropriate form of eq 15 for the overall molecular tumbling motion,[42] and using the END interaction tensor for the methyl protons, averaged over the internal motion[41] with the experimentally measured τ_R at -85 °C of 83 μs (cf. discussion of the COSY experiments above), yields a value of τ_c about 3 orders of magnitude longer than the value obtained at this temperature, i.e., $\tau_c \approx 30$ μs. Also, as the temperature is reduced further, this spin-flip rate will decrease as $W_n \propto \tau_R^{-1}$ in this regime, in contradiction to experiment. [Note that the validity of an equation like eq 15 in the slow motional regime, although derived for the fast motional regime, has been verified by Schwartz.[7]]